

Design and Development of Highly Torque Dense Robot Joint Using Flexible Shaft Based Remote Actuation

Muhammad Usman^{*,1,3}, Thierry Hubert^{1,2}, Amin Khorasani^{1,2}, Raphaël Furnémont^{1,2},
Bram Vanderborght^{1,3}, Dirk Lefeber^{1,2}, Greet Van de Perre^{1,3} and Tom Verstraten^{1,2}

Abstract—Remote actuation is an important design technique to reduce the moving mass of robots for safety. This paper proposes a remote actuator based on the flexible shaft for robot joints. High torque density is achieved at the robot joint, rated at 95 Nm with a low moving mass of 2.6 kg (1.8 kg at Joint + 0.8 kg at Link). The design methodology is proposed to develop a remote actuator using a flexible shaft with low-moving mass and torsional compliance at the remote joint with three progressive prototypes. The design of the conduit and link utilized for routing flexible shaft across a joint through the links is analyzed and discussed. A comparison is made with on-joint actuation and potential off-joint actuation using catalog data in terms of torque density, highlighting the potential of remote actuation using a flexible shaft for high payloads at high torque density.

I. INTRODUCTION

Safety in Human-Robot Interaction is a growing demand in the field of modern robotics. Active and passive compliance has been introduced in the robots to ensure their safe operation around humans [1] [2]. Apart from compliance, another perspective in achieving safety has been achieved by reducing the robot's inertia using remote actuation based on cable-driven systems [3] [4] [5] [6]. Cable-driven actuation due to their flexibility, low inertia, low noise and high sensitivity offer many design benefits. Developing 7 DOF manipulators equal in size and mass to the average Human arm is a task achievable using cable-driven actuation [4] [7]. The lowest value of 2.87 kg is achieved in [6] at the cost of low stiffness. Tension amplification systems are proposed in [4] [5] to attain comparable stiffness with regard to industrial or on-joint actuation robots. However, the payload capabilities are limited in comparison to humans and industrial robots using cable-driven systems in a serial configuration, reporting payload up to 3-5 kg [3] [4].

To attain higher payloads with high torque density, remote actuation systems such as cable or belt pulleys have not been a favorable choice due to their increased pulley sizes and cable/belt dimensions. Thus, for the high payload, the series configuration of actuation using cables is not suitable, leading to parallel robot structures driven by cables [8]. Also, by increasing the payload, the non-linear extension of cables and belts increases the complexity of tensioning

mechanisms. A high payload, though achievable by belt-pulley systems, comes at the cost of a bigger volume than a human arm, and it is being utilized in KUKA heavy payload industrial robots KR 500 series [9].

Cianca et al. [10] introduced a remote and torsionally compliant actuator for wearable robots using flexible shaft. The flexible shaft's compliance with bending torsion provides the design benefit of being routed remotely to deliver torque at the distal location. Owing to its combined advantages of elasticity and remote actuation, it has found different applications in robotics, such as a surgical robotic manipulator [11], a novel soft actuator [12] and a search robot actuated by flexible shafts [13]. Flexible shafts have also been used as compliant remote actuation in medical applications like endoscopy, colonoscopy, and surgical robot tools [14]. Flexible shafts, being rotary actuators, suit human assistance devices more than linear forces actuators, where the transmission is performed from the waist to ankle [15] and trunk [16], along the human body compactly and safely. This demonstrates the versatility of the flexible shaft as the transmission for remote actuation systems.

This research focuses on using flexible shafts as a remote and elastic transmission for robot joints with high payloads where the utility of cable-driven and belt-pulley actuation offers design complications. The actuation system based on a flexible shaft is designed for a distal robot joint of the elbow in a serial 3-DOF anthropomorphic arm configuration. The design objectives are to achieve low moving mass and high compactness with simplicity in design compared to the counterparts of on-joint and off-joint actuation systems. A series of prototypes are designed to augment and explore the capabilities of flexible shafts as a remote transmission, leading to a final prototype of high torque density. The iterative design is discussed and analyzed with experimental results, entailing the benefits of each iteration. The final prototype is compared with on-joint and off-joint actuation systems with the catalog data to highlight its potential. The main contribution lies in proposing a light-weight high torque density robot joint based remote actuation using flexible shafts, with methodology to design it.

This paper is organized as follows: Section II discusses the overall design approach for the remote actuator, along with the characteristics of a flexible shaft as a transmission. Section III discusses the design iterations from prototype to prototype, alongside their experimental evaluation. Section IV discusses the outcomes by comparing the actuator with on-joint and off-joint counterparts to conclude the paper.

This research is supported by Research Foundation Flanders (FWO) SBO project ELYSA Project (grant number S001821N).

The authors are affiliated with: ¹ Brubotics, Vrije Universiteit Brussel, Brussels, Belgium. ² Flanders Make, Brussels, Belgium. ³ Imec, Brussels, Belgium.

*Corresponding author: muusman@vub.ac.be (Muhammad Usman)

II. REMOTE ACTUATION DESIGN AND ANALYSIS

The main objective of remote actuation is to reduce the moving mass of the robot, relocating it to the robot's base. This section discusses the characteristics of flexible shafts, which inform the design of remote actuators. The design of the remote actuator is discussed afterward with different possible configurations, where the aim is to deliver torque across a robot joint to a distal joint.

A. Flexible Shaft

A flexible shaft is an elastic slender rod made of twisted coils wrapped around each other in opposite directions of helices, as shown in Figure 1 (a) and (b). It is constructed using twisted wires at the core enclosed by the multiple coils back to back for wrapping the twisted wires till the desired diameter is achieved with multiple layers of coils. The direction of the helices of the coils is kept opposite from layer to layer, restraining the unwinding of coils on the application of bi-directional torque. The selection of wire diameter and diameter of the flexible shaft is made based on the amount of torque to be delivered using a flexible shaft. The helix angle of the twisted wires at the center is kept high to promote linear tension strength. On the contrary, the helix angles of the coil are kept smaller to ensure high torsional strength. The shaft has torsional and bending compliance, making it useful for the transmission of torque across obstacles for different applications. This potential of a flexible shaft makes it a viable element for remote actuation, which inherently possesses elasticity as an added advantage.

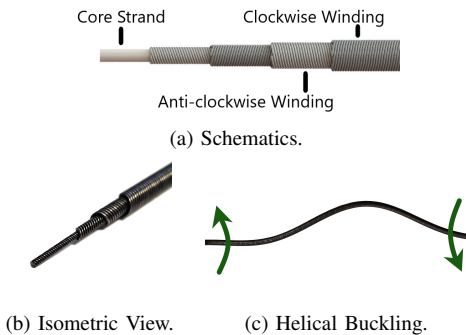


Fig. 1. Flexible Shaft Construction and Characteristics.

Once a torque is applied to a flexible shaft, the coils in the direction of torque tightly wind to compress the internal coils, while the coils in the opposite direction of torque unwind to compress the outer coils. This generates internal resistance to handle torque delivery across an obstacle. An outermost coil of the flexible shaft, being uni-directional, can either be in the direction of torque or against it, making the characteristics of the flexible shaft asymmetrical in both directions. Suppose the magnitude of torque applied on the flexible shaft keeps increasing. In that case, it results in helical buckling deformation, as shown in Figure 1 (c), where the inability of coils to retain their shape is reached. This limit is called critical torque, around which the nominal

ratings of the flexible shaft are defined. Further, an increase in the torque results in a collapse with high forces generated at both connection points. A thick and short flexible shaft is less prone to helical buckling [17], capable of delivering high nominal torque similar to a rigid shaft. Increasing the diameter of the flexible shaft would result in a nearly rigid shaft with a very high bending stiffness, making it not viable for remote solutions where overcoming an obstacle is important, like a robot joint.

B. Actuator Concept

A remote actuator design aims to position the motor remotely and overcome obstacles, particularly in robot joints for torque delivery. A generic configuration, shown in Figure 2, is adopted, employing gearboxes before and after the flexible shaft to meet speed-torque demands. Three possible configurations stem from this setup, briefly outlined below:

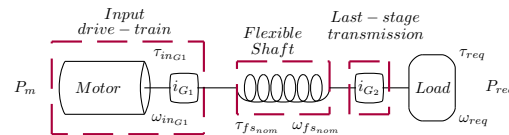


Fig. 2. Schematics of General Remote Actuation Module.

1) *Configuration A*: Configuration A is with high transmission ratio i_{G2} at the load side and no transmission at the motor side, i.e. $i_{G1} = 1$, as shown in Figure 2. The high transmission ratio at the load side makes the selection of a thinner flexible shaft with low bending stiffness and increased workspace capability. Meanwhile, the resultant gearbox asks for an increased mass in a distal location, which increases the moving mass. This goes against the design objective at hand for remote actuation.

2) *Configuration B*: Configuration B is with high transmission ratio i_{G1} at motor side and no transmission at load side i.e $i_{G2} = 1$, as shown in Figure 2. As the motor side consists of a high ratio gearbox, the weight is well placed near the motor, fulfilling the inertia reduction purpose of remote actuation. However, the output torque to be transmitted through a flexible shaft is higher, requiring a thicker and higher stiffness shaft, making it useful for applications with limited workspace requirements due to its limitation in bending. The direct contact of the flexible shaft with the load avoids the reflected inertia due to the input drive train. Robot joints being designed for high reachability will not suit this configuration.

3) *Configuration C*: Configuration C is with distributed transmission ratio at motor and load side as shown in figure 2. In comparison to configurations A & B, if the same output torque is being transmitted, configuration C facilitates a reduction in gear ratios, making the gearboxes lighter, whether at the motor or load end. This trade-off in the transmission provides a balance in the workspace capability of the flexible shaft and output stiffness at the load end. However, on the other side, the increase in the number of components adds

to the mechanical complexity, leading to more losses and maintenance issues with additional cost value. This price is generally feasible to pay at the motor end, and dedicated care can be provided for the distal load end transmission design. A transmission system with high efficiency and mechanical simplicity can favor this configuration to be useful for robots with large workspaces.

C. Design Process

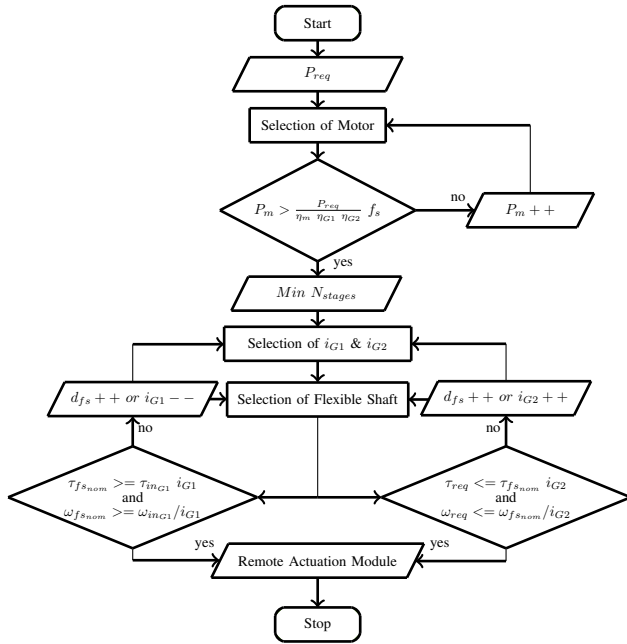


Fig. 3. Design Process of Remote Actuation Module: Configuration C.

Configuration C is selected for the design of our remote actuator due to the benefits of a better workspace and possible reduction of moving mass. Figure 3 shows the development process of this configuration. The process starts with the selection of a motor based on the required rated output mechanical power P_{req} . The safety factor f_s for the electrical power rating of the motor compensates for the mechanical and electrical losses from the motor to the load end. For the selection of gearbox G_1 and G_2 , the constraint of a minimum number of stages, N_{stages} is applied to constitute the constraint of minimum possible gear ratios. The priority is to achieve a minimum number of stages, N_{stages} at the load end to reduce effectively the moving mass. Followed by the selection of gearboxes, the selection of flexible shaft is performed based on its nominal torque $\tau_{fs_{nom}}$ and minimum bending radius to achieve a joint range of $\pm 90^\circ$. The required torque τ_{req} and speed ω_{req} are achieved by meeting the kinematic constraints introduced by the gear ratios i_{G1} and i_{G2} . There are two separate decision paths for each gearbox where the objective is to decrease the gear ratio of G_1 and increase the gear ratio of G_2 . This is adopted to attain the desired joint range using the selected flexible shaft. Alternatively, the diameter d_{fs} of the flexible shaft is increased to allow higher torque transmission through the shaft at the expense of a higher bending radius.

III. MECHANICAL DESIGN AND EVALUATION

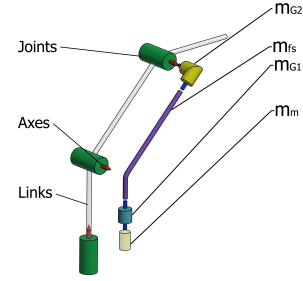


Fig. 4. Robot Configuration.

To demonstrate the high payload capabilities of the flexible shaft, a three DOF robot configuration, as shown in Figure 4, is considered to match the kinematics of KUKA LBR IIWA with a payload of 14 kg for the initial two prototypes. Here, the elbow joint is remotely actuated with a rated torque of 52 Nm (peak 66 Nm) at 75 deg/s. For the final prototype, the rated torque of 95 Nm at 75 deg/s is considered to scale up the payload to 18 kg. To design the remote actuation, the experimental setup and prototypes developed with their findings are discussed below.

A. Experimental Setup

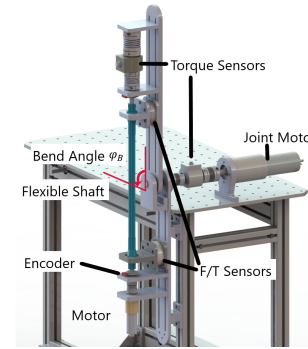


Fig. 5. Experimental Setup.

Figure 5 shows the experimental setup used for the evaluation of the flexible shaft of each prototype. A Maxon brushless DC motor (Catalog no. 167178) with a planetary gearbox (Gear ratio 91:1, catalog no. 203125) is used as a torque source. A DBRK-20 analog torque sensor (ETH-Messtechnik) with a measurement range of 20 Nm is used for the torque measurement of the flexible shaft. The torque sensor is fixed at the load end, and its other end is connected with a flexible shaft's end fitting. An optical encoder EM2 from US Digital is used between the motor's output and the input of the flexible shaft to measure the twist angle of flexible shafts. For bending, a maxon brushed DC motor (Catalog no. 353295) with a planetary gearbox (Gear ratio 51:1) is connected through a torque sensor to the joint between two links as shown in Figure 5. This joint motor achieves different bending angles or deflection, φ_B , as shown

in Figure 5. For data acquisition, Beckhoff IO modules are used alongside the Maxon Driver EPOS4, integrated with TwinCAT EtherCAT. All these components are connected through bellow shaft couplings to compensate for the rotation axis misalignment with no backlash. The ends of the flexible shaft are fixed to restrict any linear contraction due to helical buckling. A set of multi-axis Force/Torque sensors is used before and after the flexible shaft for measuring the structural loads. An input signal for desired torque τ for each flexible shaft is fed to the torque controller. The amplitude of desired torque signals is selected based on the nominal torque of each prototype's flexible shaft. The exact desired torque profile is followed for the bending angles of each flexible shaft varied from $\varphi_B = 0^\circ$ to 90° with 15° step in between. Implementation is done using MATLAB Simulink and TwinCAT shell for Microsoft Visual Studio.

B. Prototype 1 - Flexible Shaft Without Conduit

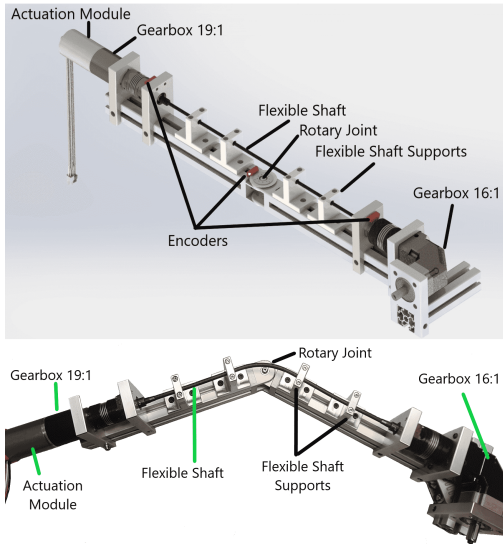


Fig. 6. Prototype I - Flexible Shaft Without Conduit.

1) *Design*: The main components of the prototype are shown in Figure 6 with details mentioned in Table I. As per the generic schematic shown in Figure 2, two sets of gearboxes are optimized in ratios to have minimum stages and least distal mass before and after the flexible shaft. A planetary + bevel gearbox combination is used for the i_{G_2} with the value of 16:1, weighing 2.1 kg with a rated torque of 45 Nm. Among the manufacturers of right angle transmissions, i.e., Neugart, Wittenstein, and Nidec, to name a few, ApexDynamics Inc. is selected for their low weight and high efficiency in comparison with other manufacturers for gearbox G_2 at the load end. A maxon's ceramic planetary gearbox with the value of $i_{G_1}=19$ is used in combination with 180 W EC motor. EC motors from Maxon are explicitly considered due to their better efficiency. In order to select an optimized motor for the remote actuation module, all the motors in the range of the required electrical power, i.e., 170-200W, are considered with safety factor $f_s = 1.3$. To

utilize the benefit of flexible shaft as an in-built torque sensor, a set of incremental encoders from US Digital with 8000 CPR are used before and after the flexible shaft to measure the amount of torsional deflection for an output torque. The components are connected using bellow shaft couplings to avoid misalignment. Angular contact bearings are selected to disconnect the radial and axial forces generated by the deformation of the flexible shaft from the motor end and gearbox end. The flexible shaft is supported along the length with aluminum supports with Igus iglidur plastic bearings to route it across the bend of the rotary joint.

TABLE I
PROTOTYPE I SPECIFICATIONS.

Actuation Module Parameters					
Nominal Torque	6.6	Nm	Nominal Voltage	48	V
Nominal Speed	27.28	rad/s	Nominal Current	4.6	A
Mass, m_m	1.4	kg	Gear ratio	19	/
Flexible Shaft Parameters					
Nominal Torque	4.8	Nm	Torsional Stiffness	0.8	Nm/rad
Nominal Speed	209.4	rad/s	Maximum Deflection	0.5	rad
Mass, m_{fs}	0.5	kg			
Right Angle Transmission Parameters					
Nominal Torque	45	Nm	Nominal Speed	1.31	rad/s
Mass, m_{G_2}	2.1	kg	Efficiency	95	%

To select the flexible shaft for the actuator, the catalog of SSWHITE UK [18] has been studied in detail, relating the trends of change in dimensions with to the properties of interest such as rated torque, speed, minimum bending radius, torsional, and bending stiffness, etc. Among these properties, the rated torque and minimum bending radius are considered as they play an essential role in achieving the required actuation. The rated torque increases non-linearly with respect to the diameter of the flexible shaft [17] [18]. Increasing the thickness of the flexible shaft makes the flexible shaft behave like a rigid shaft, which can handle more nominal torque with the least bending or torsion possible. Considering the nominal torque and bending stiffness of the flexible shafts and their output torque, a flexible shaft with a diameter of 8 mm and a length of the flexible section of 450 mm with end fittings at both ends, making the total length 525 mm. The length of flexible shafts is chosen based on the second link's length of the 3-DOF robot. The total mass of the actuator module, excluding the aluminum strut profiles used, is 4.083 kg, where the mass distribution is $m_m = 1.443$ kg (G_1 with Maxon motor) at the motor end, $m_{fs} = 0.54$ kg of the flexible shaft, and $m_{G_2} = 2.1$ kg (G_2) at the load end.

2) *Experimental Evaluation*: Figure 7 shows the characteristics at various bending angles ranging from 0° to 90° . The characteristics show an almost linear behavior for low bending angles till 30° . Beyond the 30° bend angle, the flexible shaft undergoes helical buckling, making the input-output characteristics highly non-linear with a pull force

of 46.4 N at 3.5 Nm torque, on the motor and load ends. This highlights that the critical torque for helical buckling is achieved at low values for high bending angles. Any torque lower than critical torque, which is almost 1 Nm, seems to be a feasible torque to transmit using the flexible shaft of the prototype I for bending angles higher than 30°. The helical buckling starting point is highlighted in Figure 7.

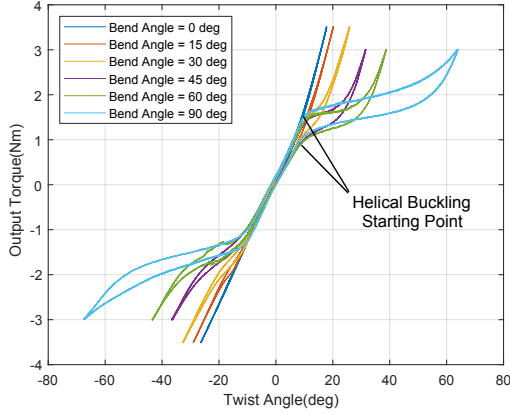


Fig. 7. Input Output Characteristics of Flexible Shaft - Prototype I.

C. Prototype II - Flexible Shaft With Conduit and Planar Link

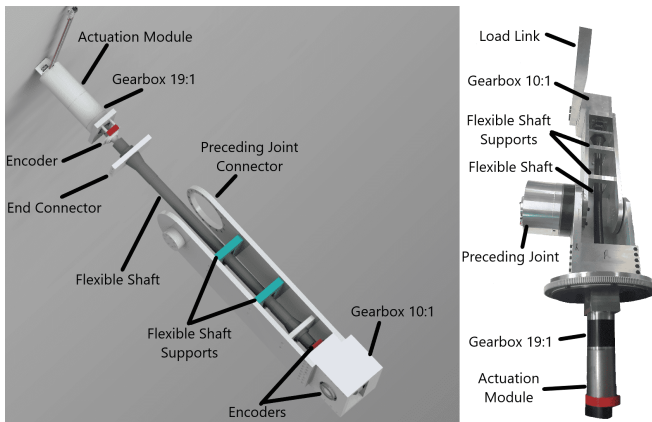


Fig. 8. Prototype II - Flexible Shaft With Conduit and Planar Link.

1) *Design*: The main components of the prototype are shown in Figure 8 with details mentioned in Table II. Following Figure 3, the development process of the remote actuation module is the same as prototype I. In contrast to prototype I, the flexible shaft with a conduit is selected, and the robot link is designed with shaft supports. A flexible conduit with low bending stiffness and high torsional rigidity is being used, made of coil tube enforced with a sheath to avoid extension during bending. It helps the design of the robot link without the use of multiple supports along the length, as in the case of Prototype I. The conduit also adds to the stiffness of the flexible shaft with geometric constraints around it, restraining helical buckling. This leads to higher

torque ratings for the same diameter of the flexible shaft by pushing the critical torque to a higher value.

TABLE II
PROTOTYPE II SPECIFICATIONS.

Actuation Module Parameters					
Nominal torque	7.9	Nm	Nominal voltage	48	V
Nominal speed	27.3	rad/s	Nominal current	4.9	A
Mass, m_m	2.1	kg	Gear ratio	19	/
Flexible Shaft Parameters					
Nominal torque	14.1	Nm	Torsional stiffness	15.3	Nm/rad
Nominal speed	209.4	rad/s	Maximum deflection	0.5	rad
Mass, m_{fs}	0.9	kg	Efficiency	80	%
Right Angle Transmission Parameters					
Nominal torque	52	Nm	Nominal speed	1.31	rad/s
Mass, m_{G2}	3.2	kg	Efficiency	90	%

The conduit design is investigated using two different modalities shown in Figure 9. Due to the helical buckling of the flexible shaft, in modality A, the generated pull force F_l gets distributed evenly onto the robot structure through bearings. However, for modality B, the force, F_l , impacts the joint directly, which demands an additional structural mass. An increase in the inner diameter of the conduit leads to the allowance of more helical buckling. Hence, a minimal difference of $d_c/2 = 2$ mm is kept between the outer and inner diameter of the flexible shaft and conduit after testing at different conduit's inner diameters. Modality A is utilized in the design due to better structural pull distribution.

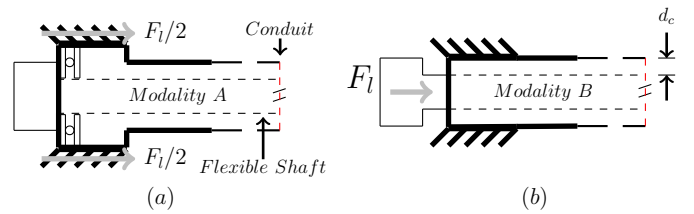


Fig. 9. Flexible Shaft Conduit Design.

The link design of the robot with a flexible shaft is analyzed with respect to routing and structural loads. Due to the flexibility of the flexible shaft, it generates out-of-plane forces and moments when torque is being transferred. Due to this nature, a couple of multi-axis F-T sensors are used to analyze the loads on the link structure. With regard to the routing of the flexible shaft, a single curvature bend in a plane is restrained to avoid a decline in the efficiency of the flexible shaft's transmission, as shown in Figure 10. Importance should be given to the placement distance of the supports as they define the nature of curvature for a flexible shaft with a specific diameter and length. Figure 10 shows the effect of change in distance from the joint axis on the curvature type of flexible shaft. The shaft takes a multi-curvature path for closely spaced supports toward the joint

axis as it gets constrained due to the supports. However, the flexible shaft takes a single-curvature path for supports away from the joint axis. The single curvature makes the flexible shaft avoid additional contact with its casing along the length and helps it bend naturally. This leads to a reduction in friction between the shaft and the casing. Slot distance, as shown in Figure 10, is important to achieve natural bend at maximum bending radius, usually two times the outer diameter of the conduit.

A further investigation is done to choose an optimal right angle transmission for a flexible-based remote actuator using [19]. Among the candidates of planetary+bevel, bevel, worm, and hypoid gearboxes, a hypoid gearbox is selected for its better efficiency, simplicity, and compactness. The planetary + bevel gearbox is not used anymore due to its multi-stage nature and centerline offset, which increases the width of the joint. Worm gearboxes, usually known for self-locking characteristics, are not a good choice for good efficiency. Even after adjusting the pitch angle of the worm to attain low friction, the worm gearbox offers less efficiency due to its nature of sliding friction-dominant teeth meshing. The bevel gear delivers torque using an engagement of single teeth at a time, which requires an increase in size with the increase of nominal ratings, leading to an increase in mass more than a hypoid gearbox.

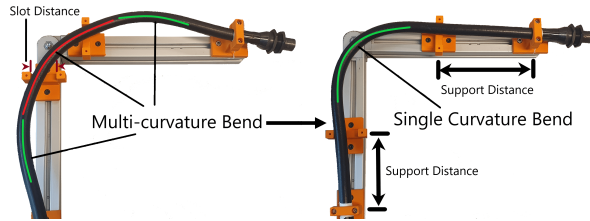


Fig. 10. Supports Design for Maximum Bending Radius and Single Curvature.

The proposed remote actuation module has a total mass of 5.1 kg, distributed along the robot with the main chunk of mass at both ends of the flexible shaft. The mass of the motor with gearbox is $m_m = 2.1$ kg, located at the preceding link, so it is not a part of the moving mass as per the robot configuration in Figure 4. The mass of the flexible shaft is $m_{fs} = 0.9$ kg, which is distributed at the link length of 50 cm. As per the dimensions of the flexible shaft in link 2, the added moving mass due to the flexible shaft is 0.63 kg (70% m_{fs}). The mass of the hypoid gearbox is $m_{G2} = 3.2$ kg, which is considerable. The main objective in this iteration was to achieve a customized, highly efficient right-angle transmission without mass optimization, which is fairly achieved at 90 % efficiency.

2) *Experimental Evaluation:* Figure 11 shows the benefits of using a flexible shaft with a conduit as the characteristics are nearly linearized, and high torque transmission is possible using the same diameter and length of the flexible shaft. There is a slight change in the stiffness values over the bending angle, with an increasing hysteresis region. The asymmetrical nature of the flexible shaft for the torque in

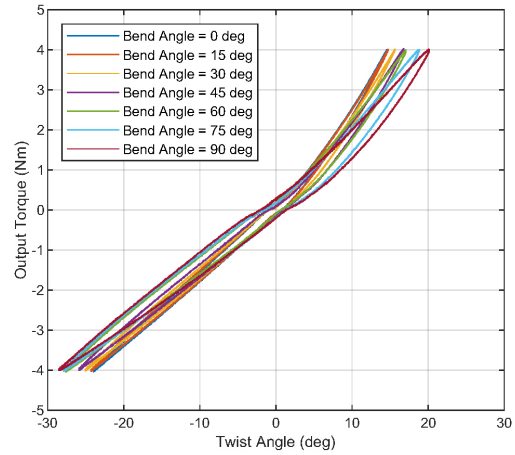


Fig. 11. Input-Output Characteristics of Flexible Shaft - Prototype II.

the direction or opposite to the outermost coil's winding can be noticed. A considerable linearization and augmentation of nominal torque capability for high bending angles is achieved using a conduit around a flexible shaft to restrain helical buckling with bearings at both ends (modality A).

D. Prototype III - Flexible Shaft With Conduit and Cylindrical Link

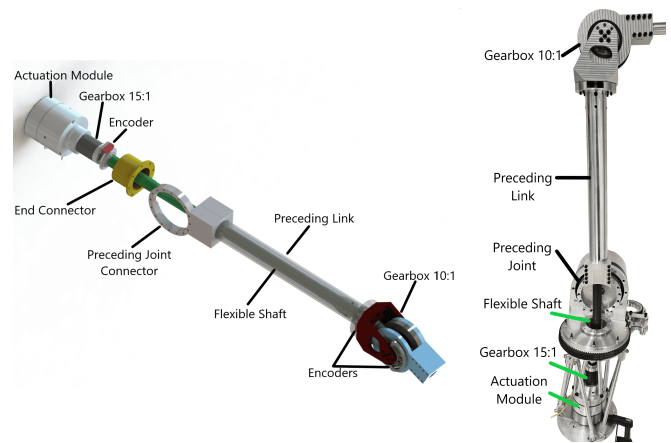


Fig. 12. Prototype III - Flexible Shaft With Conduit and Cylindrical Link.

1) *Design:* The main components of the prototype are shown in Figure 12 with details mentioned in Table III. To simplify the link design, a cylindrical link is used instead, where support distance and slot distance are not required at the cost of a slightly lower bending radius. To achieve low moving mass, the hypoid gearbox is optimized using thin section 4-point contact bearings and customization of NIDEC hypoid gear and pinion for the robot joint. A considerable mass reduction is achieved with a high torque rating of 95 Nm in comparison to 52 Nm in previous iterations. The actuation module is optimized in mass to be the same as prototype II with the addition of a Miki pulley brake installed, which is essential for safety considerations. A 12

Nm flexible shaft is taken with an additional length of 50 mm in comparison to support the high payload.

TABLE III
PROTOTYPE III SPECIFICATIONS.

Actuation Module Parameters					
Nominal Torque	11.5	Nm	Nominal Voltage	48	V
Nominal Speed	16.4	rad/s	Nominal Current	4.9	A
Mass, m_m	2.1	kg	Gear ratio	15	/
Flexible Shaft Parameters					
Nominal Torque	12.1	Nm	Torsional Stiffness	16.85	Nm/rad
Nominal Speed	314.15	rad/s	Maximum Deflection	1.48	rad
Mass, m_{fs}	1.2	kg	Efficiency	80	%
Right Angle Transmission Parameters					
Nominal Torque	95	Nm	Nominal Speed	1.64	rad/s
Mass, m_{G2}	1.8	kg	Efficiency	85	%

The final remote actuation module has a total mass of 5.1 kg, the same as prototype II. The mass of the motor with gearbox and brake is $m_m = 2.1$ kg. The mass of the flexible shaft is $m_{fs} = 1.2$ kg, distributed at the link length of 50 cm. As per the dimensions of the flexible shaft in link 2, the added moving mass due to the flexible shaft is 0.84 kg (70% of m_{fs}). The mass of the hypoid gearbox is $m_{G2} = 1.8$ kg, which is a significant reduction in increasing the torque density of the robot joint. This makes the moving mass of 2.6 kg ($0.7 * m_{fs} + m_{G2}$).

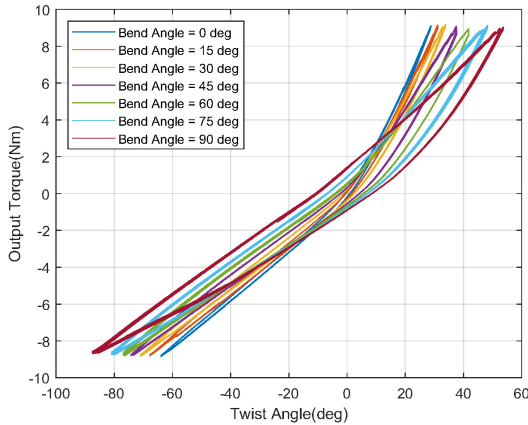


Fig. 13. Input Output Characteristics of Flexible Shaft - Prototype III.

2) *Experimental Evaluation:* Figure 13 shows the characteristics of the flexible shaft utilized for this revision, which is similar to prototype II. There is an increase in hysteresis region due to more torsional deformation of the flexible shaft under the effect of bending. A hysteresis compensation is required for such differences in input and output's rising and falling curves. A pull on motor and load end of $F_l = 161$ N, distributed around the cylindrical link. This structural load is important to consider for designing optimized weight link.

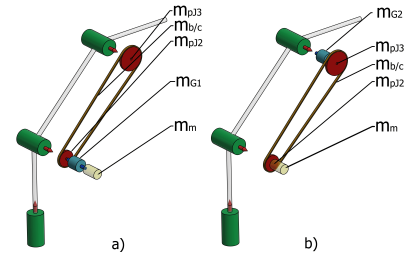


Fig. 14. Remote Actuation based on Belt-Pulley System.

3) *Comparison of On-Joint and Off-Joint Actuators:* For a fair comparison with the developed remote actuator, catalogs of available on-joint actuators are checked with nominal torque (maximum continuous torque) and speed ratings around the design ratings. On-joint actuators designed for robots usually have nominal speed ratings of 1.3-3.14 rad/s. Hence, nominal torque rating is used for comparison instead of power ratings. Without brake, joint modules are considered for fair mass comparison.

TABLE IV
COMPARISON OF ON-JOINT WITH OFF-JOINT ACTUATORS.

Company	Model	Actuation Type	Rated Torque (Nm)	Joint Mass (kg)
Harmonic Drive ®	IHD-25A	HarmonicDrive + Motor	119	4.3
Spinbotics	DB-03	HarmonicDrive + Motor	85	2.75
Umbratek	HR-A086	HarmonicDrive + Motor	72	2.9
Sumitomo	Tuaka Servo	HarmonicDrive + Motor	67	2.4
AROS ABSIS	D90	HarmonicDrive + Motor	62	1.7
VUB	Prototype III	Flexible Shaft	95	1.8
Mitsuboshi+ Neugart + Maxon	S8M+ PLE+ IDX70M	Belt Pulley + Planetary Gears + Motor	95	1.8
Neugart + Mitsuboshi + Maxon	PLE+ S5M IDX70M	Planetary Gears Belt Pulley + Motor	95	2.95
Harmonic Drive®+ Mitsuboshi+ Maxon	CSG-2UH + S5M+ IDX 70M	Harmonic Drive Belt Pulley + Motor	95	2.55

For the case of off-joint actuation, a set of components is required to synthesize the whole remote actuation. Figure 14 shows the simplest possible configurations of the belt-pulley systems-based remote actuation modules without a tensioning mechanism (i.e., idler pulleys). Figure 14 (a) utilizes a gearbox before the belt-pulley system, while Figure 14 (b) utilizes a gearbox after the belt-pulley system. These configurations help the belt-pulley system achieve a high transmission ratio. Two types of gearboxes are used for scenario 14 (b): harmonic drive and planetary gearbox. This construction is easily be utilized for the cable-pulley arrangement, as the ratings of component will remain the same.

Table IV shows the on-joint mass in the case of on-joint and off-joint actuation. The green row shows prototype III, and the yellow row shows the closest candidate based on the belt-pulley system. A fair difference in mass can be observed along with a higher nominal torque rating, demonstrating the high-torque density of the flexible shaft-based remote actuator. Belt pulley system-based off-joint actuators offer an equivalent joint-mass solution without considering the weight of tensioning mechanism.

IV. DISCUSSION AND CONCLUSION

Three flexible shaft-based remote actuation modules are discussed, along with their input-output characteristics. Without a conduit, the shaft experiences helical buckling at low torques, suitable only for small payloads. Adding a conduit prevents buckling, linearizing its characteristics and increasing nominal torque. Conduit and link design are crucial for balanced loads and high efficiency. Modality A works best with a small conduit-flexible shaft diameter difference (around 2 mm). Achieving a single planar curvature in the link design is important, requiring optimization of support placement based on shaft dimensions. A cylindrical link simplifies this, achieving curvature without supports.

For a robot design, it is essential to load the robot near to its center line to avoid torsion load on its structure. This requires a symmetrical and compact design of robot joints where on-joint actuators do not favor it, leading to more structural loads and mass. A right angle transmission being single-stage as hypoid gear with its compactness offers a compact and symmetrical robot joint design for the flexible shaft. A robot joint based on a hypoid gearbox is designed for a 95 Nm rating with a mass of 1.8 kg (including connectors for the load link). With its high efficiency of 85%, transparency to flexible shaft elasticity is attainable, decoupling the inertia of the actuation module in the base. These specifications are highly torque dense, as can be seen in Table IV, where on-joint actuators available in the market and remote actuation based on timing belts designed using catalog data are compared. Among the enlisted candidates, a belt pulley system offers a competitive rating at the cost of high belt tensioning with more mechanical components. The belt-pulley system gets even more heavier and complicated as it is moved down towards the base, introducing coupling between the robot joints. For the case of flexible shaft, it offers a parallel compliance on preceding joint, which can be exploited for the reduction of gravitational load.

A remote actuator design using a flexible shaft is discussed with three prototypes, showcasing its high payload capability. Each prototype explores flexible shaft characteristics. The conduit and link design accommodate natural bending and distributed load. Increased hysteresis due to shaft bending is noted, prompting future hysteresis compensation for precise torque control. Parallel compliance from the shaft reduces static torques and will be further studied. Focus on repeatability and lifecycle is crucial. The actuator will be integrated into a robot arm for pick and place tasks.

REFERENCES

- [1] G. Hirzinger, N. Sporer, A. Albu-Schaffer, M. Hahnle, R. Krenn, A. Pascucci, and M. Schedl, "Dlr's torque-controlled light weight robot iii-are we reaching the technological limits now?" in *Proceedings 2002 IEEE International Conference on Robotics and Automation (Cat. No.02CH37292)*, vol. 2, 2002, pp. 1710–1716 vol.2.
- [2] G. Pratt and M. Williamson, "Series elastic actuators," in *Proceedings 1995 IEEE/RSJ International Conference on Intelligent Robots and Systems. Human Robot Interaction and Cooperative Robots*, vol. 1, 1995, pp. 399–406 vol.1.
- [3] W. T. Townsend and J. K. Salisbury, "Mechanical design for whole-arm manipulation," in *Robots and Biological Systems: Towards a New Bionics?*, P. Dario, G. Sandini, and P. Aebischer, Eds. Berlin, Heidelberg: Springer Berlin Heidelberg, 1993, pp. 153–164.
- [4] Y.-J. Kim, "Anthropomorphic low-inertia high-stiffness manipulator for high-speed safe interaction," *IEEE Transactions on Robotics*, vol. 33, no. 6, pp. 1358–1374, 2017.
- [5] S. Pang, W. Shang, F. Zhang, B. Zhang, and S. Cong, "Design and stiffness analysis of a novel 7-dof cable-driven manipulator," *IEEE Robotics and Automation Letters*, vol. 7, no. 2, pp. 2811–2818, 2022.
- [6] Y. Tsumaki, Y. Suzuki, N. Sasaki, E. Obara, and S. Kanazawa, "A 7-dof wire-driven lightweight arm with wide wrist motion range," in *2018 IEEE/RSJ International Conference on Intelligent Robots and Systems (IROS)*, 2018, pp. 1–9.
- [7] Y. Huang, Y. Chen, X. Zhang, H. Zhang, C. Song, and J. Ota, "A novel cable-driven 7-dof anthropomorphic manipulator," *IEEE/ASME Transactions on Mechatronics*, vol. 26, no. 4, pp. 2174–2185, 2021.
- [8] M. Zarebidoki, M. Zarebidoki, J. S. Dhupia, J. S. Dhupia, W. Xu, X. Wang, and X. Lu, "A review of cable-driven parallel robots: Typical configurations, analysis techniques, and control methods," *IEEE Robotics and Automation Magazine*, 2022.
- [9] KUKA, "Kr 500 fortéc - kuka industrial robots," <https://www.kuka.com/en-be/products/robotics-systems/industrial-robots/kr-500-fortec>, 2024.
- [10] D. Rodriguez-Cianca, C. Rodriguez-Guerrero, T. Verstraten, R. Jimenez-Fabian, B. Vanderborght, and D. Lefeber, "A flexible shaft-driven remote and torsionally compliant actuator (rtca) for wearable robots," *Mechatronics*, vol. 59, pp. 178–188, 2019. [Online]. Available: <https://www.sciencedirect.com/science/article/pii/S0957415819300418>
- [11] Y. Sekiguchi, Y. Kobayashi, Y. Tomono, H. Watanabe, K. Toyoda, K. Toyoda, K. Konishi, M. Tomikawa, M. Tomikawa, S. Ieiri, K. Tanoue, M. Hashizume, and M. G. Fujie, "Development of a tool manipulator driven by a flexible shaft for single port endoscopic surgery," *IEEE*, 2010.
- [12] N. Tan, X. Gu, and H. Ren, "Design, characterization and applications of a novel soft actuator driven by flexible shafts," *Mechanism and Machine Theory*, 2018.
- [13] R. Hayashi, K. Nicho, Y. Yu, Tetsuya Kinugasa, and H. Amano, "Small search robot consisting of plural driving wheels connected by flexible shafts," *Journal of Robotics and Mechatronics*, vol. 26, no. 4, pp. 469–476, 2014.
- [14] D. Kim, D. Lee, S. Joe, B.-I. Lee, and K.-J. Cho, "The flexible caterpillar based robotic colonoscope actuated by an external motor through a flexible shaft," *Journal of Mechanical Science and Technology*, vol. 28, no. 28, 2014.
- [15] E. Tanaka, K. Muramatsu, K. Watanuki, S. Saegusa, and L. Yuge, "Walking assistance apparatus enabled for neuro-rehabilitation of patients and its effectiveness," *Mechanical Engineering Letters*, vol. 1, pp. 15–00 530–15–00 530, 2015.
- [16] H. Ooki, S. Yokota, A. Matumoto, D. Chugo, S. Muramatsu, and H. Hashimoto, "Development of walking assistance orthosis by inducing trunk rotation using leg movement: 1 st report on prototype and feasibility experiment," in *Proceedings of the 20th International Conference on Informatics in Control, Automation and Robotics - Volume 1: ICINCO, INSTICC*. SciTePress, 2023, pp. 740–746.
- [17] A. R. Black III, *On the mechanics of flexible shafts*. Stevens Institute of Technology, 1988.
- [18] S. W. Technologies, "Technical characteristics of commercial flexible shafts," <https://www.sswwhite.net/copy-of-bi-directional-english>, 2020.
- [19] S. Radzevich, *Dudley's Handbook of Practical Gear Design and Manufacture, Second Edition*. Taylor & Francis, 2012. [Online]. Available: <https://books.google.be/books?id=mLUclpsfTeQC>